Int J Adv Manuf Technol (2017) 93:4371–4378
DOI 10.1007/s00170-017-0810-3

ORIGINAL ARTICLE

New method to improve the microstructure and mechanical properties of joint obtained using FSW

O. Barooni[1] · **M. Abbasi**[1] · **M. Givi**[1] · **B. Bagheri**[2]

Received: 11 April 2017 / Accepted: 17 July 2017 / Published online: 7 August 2017

Abstract Frictional heat combined with controlled forging pressure is applied during friction stir welding (FSW) to produce high-integrity, defect-free, and full penetration welded joints. Different methods have been applied to modify and enhance the different characteristics of weld obtained using FSW. In the current research, AA6061-T6 aluminum alloy workpieces were vibrated during FSW normal to welding direction while cooling intensity was also increased by application of water. Microstructure and mechanical properties of welds were investigated and compared with those friction stir welded conventionally. The results showed that the stir zone grain size decreased and weld strength, hardness, and ductility increased significantly as vibration and coolant were applied simultaneously. It was concluded that vibration increases the straining in stir zone and coolant decreases the stir zone temperature. The former has an effective role on grain refinement and the latter decreases the decomposition of Mg_2Si precipitates. Both lead to the strength and hardness increase.

Keywords Friction stir welding · Vibration · Coolant · Microstructure · Mechanical properties

1 Introduction

Friction stir welding (FSW) is a solid-state joining process in which a rotating and wear-free welding tool is traversed along the weld path between the workpieces to be joined. The rotation of the tool generates frictional heat, which causes the material to soften. The subsequent transverse motion, combined with continuing rotation of the tool, mixes the softened material in the joining area, resulting in a high-quality weld seam [1]. Friction stir welding is especially suitable for the welding of non-ferrous metals with low melting points, such as aluminum and magnesium [2].

AA6061 aluminum alloy has a great usage in industry and its welding is important. Magnesium and silicon constitute two major alloying elements of this alloy. It is a precipitation-hardened aluminum alloy and it has good mechanical properties and weldability [3]. It is commonly available in pre-tempered grades such as AA6061-O, tempered grades such as AA6061-T6 and 6061-T651. Although, AA6061-T6 is highly weldable, but a loss of strength near the weld is observed after welding, due to precipitation decomposition [4].

Different methods have been applied to improve the FS weld quality, namely microstructure, strength, and ductility. Grain size has a domineering effect on these characteristics. Various experimental and theoretical works clarified the relations between grain size and welding conditions. Welding conditions affect the heat generation during welding. Heat may lead to grain growth and increase the grains sizes. Zhang and Zhang [5] established a new Eulerian model based on solid mechanics to model the heat generation from pin and shoulder during FSW. Their results were validated through comparison with the Arbitrary Lagrangian-Eulerian (ALE) model and the experimental data. They found that the heat input increased as the rotating speed enhanced and the ratio of the heat input fluxes from the shoulder and pin keeps constant regardless of the variations of the rotating speed. Heat from welding process might lead to grain growth and deterioration of characteristics [5]. Some trails were performed to decrease the heat input and impede grain growth during FSW.

✉ M. Abbasi
m.abbasi@aut.ac.ir

[1] Faculty of Engineering, University of Kashan, Kashan, Iran

[2] Department of Mining and Metallurgy, Amirkabir University of Technology, Tehran, Iran

Submerged friction stir welding (SFSW) under water was carried out by Mofid et al. [6] to study the effect of water cooling during FSW of AA5083 Al alloy to AZ31C-O Mg alloy. The results showed that the peak temperature decreased for about 25 °C for welds made underwater and the formation of intermetallic compounds was suppressed significantly. The results also showed that the stir zone of underwater welded specimen had a much smoother interface and lower hardness with respect to sample welded without water.

Zhang et al. [7] conducted underwater FSW to improve the mechanical properties of the HAZ for an Al-Cu joint. The results showed that precipitate coarsening decreased and precipitation free zone width decreased as FSW was conducted under water. The results also indicated that the hardness of the HAZ improved. Sharma et al. [8] experimentally analyzed the effect of in-process cooling on mechanical properties and microstructure of the FSW joints developed between AA7039 aluminum alloys. The in-process cooling was employed applying coolants directed along the weld center line at about 30 mm behind the tool using a nozzle mounted on a holder perpendicular to the plate surface. Liquid nitrogen, normal water, and compressed air at 6 bar pressure were applied as coolants. Their results showed that in-process cooling decreased the grains size in the stir zone, the heat-affected and thermo-mechanically affected zones and it also decreased the size of these zones. They also observed that in-process cooling lowered the mechanical properties of the FSW joints and changed the fracture location from heat-affected zone to stir zone. Sharma et al. [8] reported that in-process cooling lowers the maximum weld cycle temperature well below the 140 °C and under this conditions, dissolution of unstable GP zones or η′ phase occurs which leads to lower volume fraction of the η′ phase. Cho et al. [9] studied the effect of cooling and welding speed on microstructure and mechanical properties during friction stir welding of extruded Al-Mg-Si aluminum billets. Two AA6082 workpieces were joined by FSW while steel fixture consisting of top fixtures and a backing plate was designed to circulate cooling water during welding and to affect the dynamic recrystallization. High translation welding speed resulted in lower grain size in the stir zone. Their results showed that as translation welding speed increased, strength increased and elongation decreased. They also found that application of coolant increased strength as well as hardness and decreased ductility.

Fratini et al. [10] studied the effects of cooling on quality of friction stir welded butt joints of AA7075-T6 aluminum alloy blanks by application of in-process water cooling treatment experimentally and numerically. Their results showed that external cooling resulted in higher weight percentage of Mg atoms and correspondingly higher density of precipitates were formed in welded joints and joint strength increased. Except increasing the cooling severity during FSW, other methods were also applied to improve the efficiency of FSW. Pitschman et al. [11] used electric current during FSW to preheat the workpiece in front of the tool. Their results showed that with application of electric current, welding speed enhanced and energy consumption reduced. Campanelli et al. [12] applied laser-assisted friction stir welding (LAFSW) to join 6-mm-thick 5754H111 aluminum alloy plates in butt joint configuration. In this process, the laser pre-heats the workpieces during the welding. They found that the laser treatment induced lower longitudinal and transverse residual stresses and higher microhardness values in the weld zone surface. Moreover, tool wear decreased and higher welding speeds were obtained by application of LAFSW.

Ultrasonic vibrations on the tool in the pin direction and perpendicular to the welding direction were employed by Amini and Amiri [13] to study the effect of ultrasonic vibrations on FSW of AA6061-T6 workpieces. The results showed that downward force reduced and weld strength and elongation increased as ultrasonic vibration was applied during welding. Rahmi and Abbasi [14] presented a new method described as friction stir vibration welding (FSVW) to improve the microstructure and mechanical properties of joint developed by FSW between AA5052 aluminum alloys. Their method included the vibration of joining workpieces in the normal direction to the welding line. Results indicated that stir zone grain size decreased and weld strength and ductility increased as FSVW was applied.

In the current research, as a new method to improve the efficiency of FSW on microstructure and mechanical properties, coolant was applied during the FSW while the workpieces were vibrated normal to welding direction. AA6061-T6 aluminum alloys were joined. Microstructure and mechanical properties of welded specimen were compared with those of specimens welded with vibration or coolant.

2 Materials and methods

AA6061-T6 aluminum alloy sheet with thickness of 3 mm was cut and specimens with dimension of 50 × 130 mm were prepared. The specimens were de-burred and cleaned of oil and grease. The specimens were fixed on fixture while longitudinal edges were butt-positioned before welding. The chemical composition of the studied alloy is presented in Table 1.

Welding tool consisted of a cylindrical shoulder from M2 steel and a trapezoidal pin from tungsten carbide. The shoulder hardness was 65 HRC. The schematic design of tool is presented in Fig. 1.

Table 1 Chemical composition of the studied alloy

Al	Mg	Si	Cr	Mn	Ti	Cu	Zn	Fe	Other
97.30	0.85	0.65	0.15	0.10	0.10	0.20	0.20	0.35	0.10

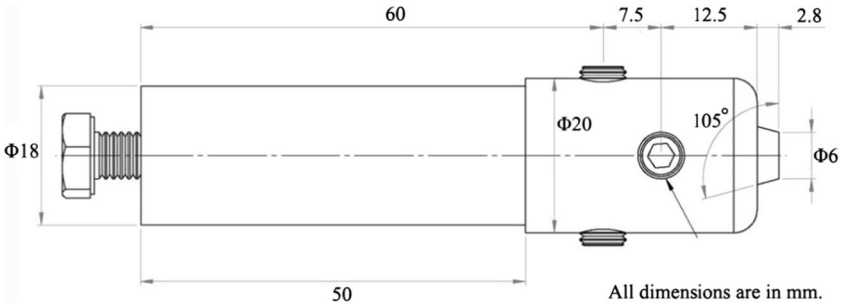

Fig. 1 Schematic design of tool used for FSW

The machine presented in Fig. 2 was designed and manufactured to apply vibration during FSW and to increase cooling intensity. Motor shaft rotation was transformed to linear and reciprocating movement of vibrating plate through a cam-shaft mechanism. Fixture was installed on vibrating plate and the joining specimens were fixed on fixture. The joining workpieces were vibrated normal to welding direction while cooling water was circuited through a canal within the fixture and under the weld line. Vibration amplitude and frequency were 0.5 mm and 60 Hz, respectively. The flow rate of water during FSW was approximately 1.9 lit/min.

Temperature record during FSW process for a fix point near the weld line was carried out by application of K-type thermocouple installed in fixture. Detailed schematic design of fixture is presented in Fig. 3. For all experiments, the rotating tool was plunged into the workpiece at a point near to the fix point. It was held there for a while without any transverse movement. When the temperature for thermocouple reached to about 140 °C, the coolant and vibration were applied and the tool was traversed. Trials showed that the temperature of 140 °C for the fix point prepares the condition for a proper welding.

Microstructure was revealed by metallographic technique based on ASTM E3-11 [15]. Keller's reagent consisted of 5 mL HNO_3, 3 mL HCl, 2 mL HF, and 190 mL H_2O was applied for about 10 s as etchant. Tensile test according to ASTM-E8 [16] was used to obtain stress-strain curves of welded specimens. Subsize specimens from welded specimens and normal to the weld line were prepared using electrical discharge machining (EDM). For each welding condition, three samples were prepared. Tensile test was carried out using the Instron 5582 Universal tester with a 100-kN load frame. Cross head speed during tensile testing was 1 mm/min.

Hardness was assessed using Vickers microhardness test according to ASTM E384 [17]. Load was 100 gf and dwell time was 10 s. For each welding condition, five measurements were obtained. Different welding trials were carried out. For all trials, tool rotation speed was 950 rpm and tool transverse speed was 50 mm/min. The grain size was quantified through the mean linear intercept method (ASTM E112 [18]).

3 Results and discussion

To completely analyze the effect of coolant and vibration during FSW, four welding conditions namely conventional FSW, FSW with presence of vibration, FSW with presence of coolant, as well as FSW with presence of coolant and vibration were considered. Cross section images of different welded specimens are shown in Fig. 4. No cracks or porosities are observed in these sections (vertical lines in these sections relate to attachment lines of pictures taken from adjacent zones by vision measuring machine (VMM) with minimum

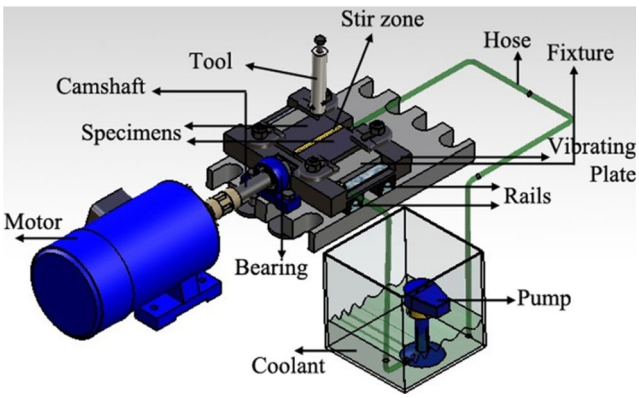

Fig. 2 Schematic design of machine manufactured for doing the welding

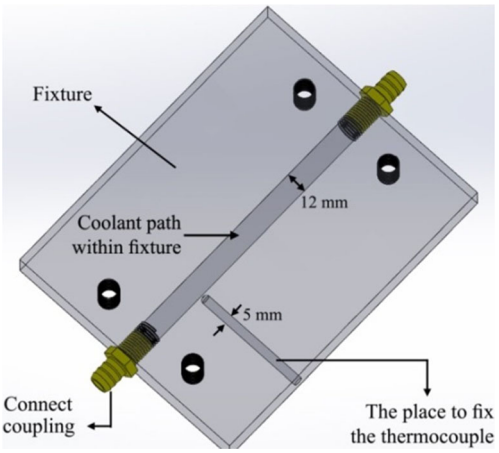

Fig. 3 Schematic design of fixture used in the experiments

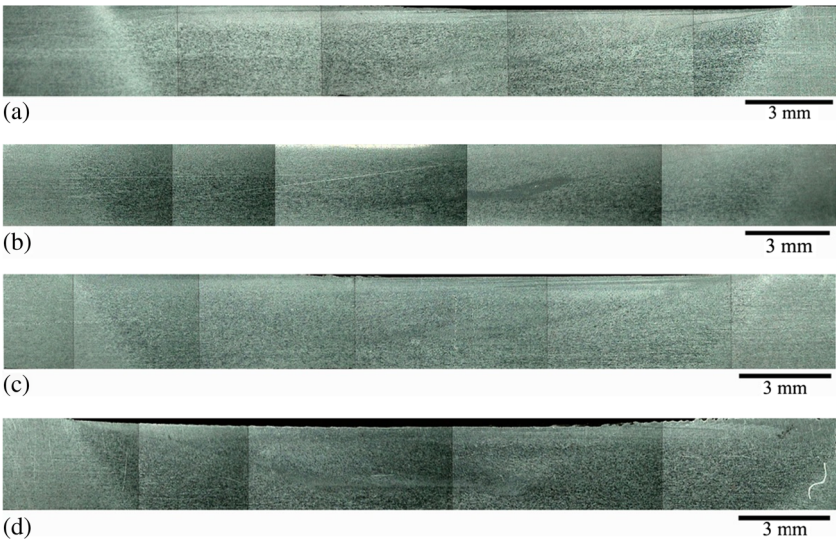

Fig. 4 Macrostructure of welded specimens: **a** FSW, **b** FSW + vibration, **c** FSW + coolant, and **d** FSW + coolant + vibration

magnification of 34). Microstructures of stir zone for different FS welded specimens as well as base material are shown in Fig. 5. It is observed that grains of the welded specimens are smaller than base material, and additionally, grains for the FS welded specimen with presence of vibration and coolant are smaller than those relating to other specimens. In Table 2, grain size values for different specimens are presented.

These can be related to vibration and coolant effects on microstructure. It is known that dynamic recovery and recrystallization are the main mechanisms for grain size control during FSW [19, 20]. According to Kaibyshev [21], three-dimensional arrays of low angle grain boundaries (LABs) are formed and gradually transform to high angle grain boundaries (HABs) during FSW as a severe plastic deformation process. Individual segments of HABs replace sub-grains evolved at small strains and accordingly grain size refinement occurs. Application of vibration results in more straining of material in the stir zone and correspondingly more dislocations are produced [22]. At high strain values, mobile dislocations move across sub-grains and result in an increase in misorientation of LABs. More HABs are formed and more grain refinement occurs [22].

Presence of coolant enhances the cooling severity and also decreases the welding temperature. According to Zener-Hollomon equation (Eq. 1) [23], Z-parameter increases, as temperature decreases. Based on Eq. 2 [24], which indicates the relation between grain size (D) and Z-parameter, grain size decreases as Z-parameter increases. So, presence of coolant restricts the growth of grains during FSW and decreases the grains sizes.

$$Z = \dot{\varepsilon}\exp\left(\frac{Q}{RT}\right) \tag{1}$$

$$D^{-1} = a\ln Z - b \tag{2}$$

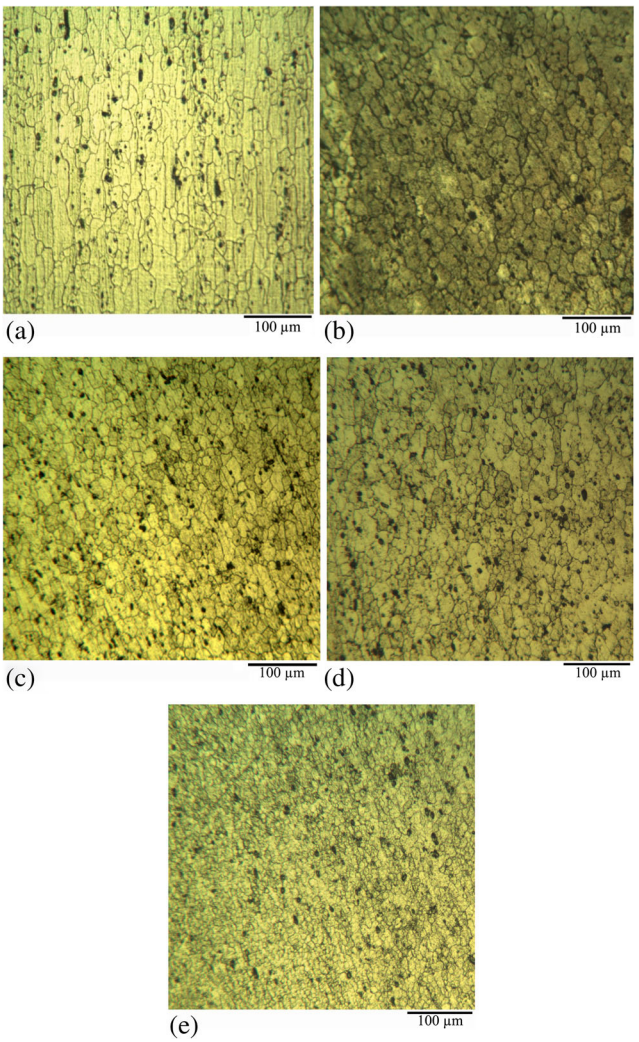

Fig. 5 Microstructures of **a** base material as well as stir zones of various welded specimens, **b** FSW, **c** FSW + vibration, **d** FSW + coolant, and **e** FSW + coolant + vibration

Table 2 Grains sizes measured for base material and stir zones of welded specimens

Specimen	Grain size
Base	47 ± 7
FSW	35 ± 8
FSW + vibration	25 ± 4
FSW + coolant	29 ± 5
FSW + coolant + vibration	12 ± 3

Temperature variation for the fix point (Fig. 3) for different welding conditions, namely conventional process, FSW with vibration, FSW with coolant, and FSW with coolant and vibration are presented in Fig. 6. For all conditions, Fig. 6 shows that temperature decreases as tool leaves the fix point (Fig. 3). It should be noted that the fix point was adjacent to the position where the welding was initiated. It is observed that temperature decreases distinctly as water is applied. It is also observed that temperature for FS welded specimen with presence of vibration is higher than that for all other specimens. Figure 6 indicates that vibration has an increasing effect on temperature. Figure 6 also shows that temperature of specimen welded using FSW with coolant and vibration is higher than that welded using FSW with coolant and lower than that of conventional FSW. It indicates that coolant effect on temperature decrease is more than increasing effect of vibration on temperature.

Minor difference among the curves at initial time in Fig. 6 relates to experimental procedure applied for detecting the temperature. For all experiments, the rotating tool at first penetrated into material without any transverse movement. When the temperature reached to 140 °C, the vibration or coolant or both were applied. So no significant difference is observed among the temperature-time curves at initial time, although the difference among the curves increases as time increases.

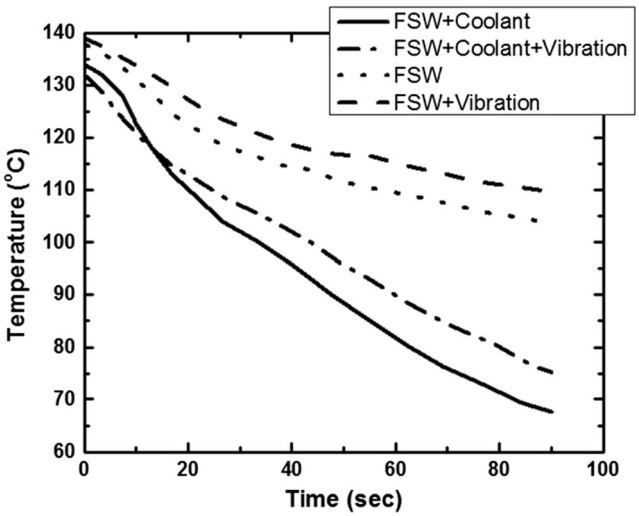

Fig. 6 Temperature variation of a fixed point (Fig. 3) adjacent to weld line for different welding conditions

Stress-strain curves of base material, conventionally FS welded specimen, FS welded specimen with vibration, FS welded specimen with coolant, as well as FS welded specimen with coolant and vibration are presented in Fig. 7. It is observed that strength and ductility of base material are higher than those of welded specimens. Additionally, the strength and ductility of specimen welded with coolant and vibration are higher than those relating to other welded specimens and mechanical properties of conventionally FS welded specimen are the least. Figure 7 also depicts that ultimate tensile strength of FS welded specimen with coolant is higher than that of FS welded specimen with vibration but its ductility is lower.

Strength drop after FSW of age-hardened aluminum Al-Mg-Si systems has been noted by different researchers [25, 26]. This is related to decomposition of Mg_2Si precipitates during welding which decreases the strength and hardness. In this regard, strength drop for welded specimens with respect to base material is reasonable.

XRD analyses results for base material as well as stir zone of conventionally FS welded specimen, FS welded specimen with coolant, and FS welded specimen with vibration and coolant are presented in Fig. 8. Although, XRD result for FS welded specimen with vibration due to its very low peaks intensities is not displayed. Analyses took place within angle range of 39.5–43.5°. Outside this range, Mg_2Si peaks are missed in background peaks due to very sharp peaks of Al. As it is observed in Fig. 8, Mg_2Si peaks intensities for base material are larger than those for other specimens and these peaks for conventionally FS welded specimen are lower than those for other welded specimens. These can be related to the effect of heat generated during welding.

Mg_2Si precipitates are constituted in microstructure of AA6061-T6 [3]. During FSW, generated heat leads to decomposition of precipitates [25]. More heat during the process results in more decomposition of precipitates. As it was seen

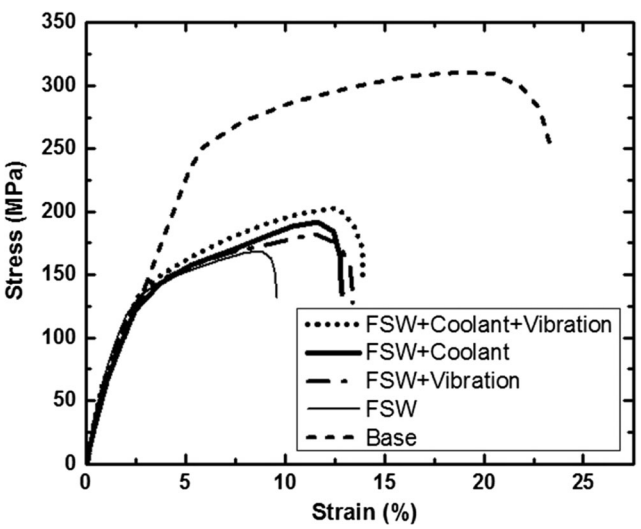

Fig. 7 Stress-strain curves of different specimens

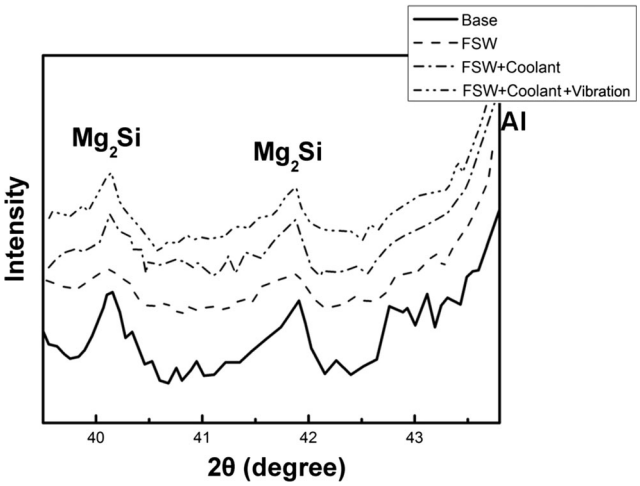

Fig. 8 XRD results for different specimens

in Fig. 6, the lowest temperature rise during FSW pertains to FSW process with coolant and the highest temperature rise relates to FSW with vibration. In this regard, high Mg_2Si peak intensities for base material and low Mg_2Si peak intensities for FS welded specimen with vibration are predictable.

It should be pointed that two strengthening mechanisms affect the strength of the studied material, precipitation hardening, and grain boundary strengthening. The precipitates act as barriers to dislocations and the degree of strengthening resulting from precipitations depends on the distribution of precipitates in the matrix. Shape, size, volume fraction, and mean interparticle spacing of precipitates are important in strengthening and these factors are all interrelated [27]. According to Orowan ($\Delta\sigma = \frac{Gb}{\lambda}$) [28], Orowan-Ashby ($\Delta\sigma = \frac{0.13Gb}{\lambda}\ln\frac{0.13Gb}{\lambda}$) [28] models the degree of strengthening ($\Delta\sigma$) depends on interparticle spacing (λ) where G and b are shear modulus and burgers vector. When some of the precipitates dissolve, interparticle spacing increases and accordingly strengthening decreases. On the other hand, grains growth increase as volume fraction of precipitates decrease. Wu and Zhang [29] modeled the grain growth process during FSW of AA6082-T6 with the consideration of pinning effect caused by precipitations using a computational fluid dynamics model coupled with a Monte Carlo simulation method. They found that with increase in temperature, the volume fraction of precipitations decrease and as a result grain growth rate and final grain size increase. The grain boundaries also act as barriers to dislocation motion and according to Hall-Petch relation ($\sigma = \sigma_0 + kD^{-\frac{1}{2}}$), strength increases as grain size decreases [30].

During FSW, dislocations are generated and arrange as new grain boundaries with high angle and as a consequence grain size decreases [19, 20]. So, FSW in one hand dissolves the precipitates which may lead to grain growth and on the other hand decreases the grains size due to dynamic recrystallization (Table 2). While the former has a decreasing effect on strength, the latter one has an increasing effect on strength.

During FSW with coolant, temperature decreases significantly and less precipitates dissolve in the matrix with respect to conventionally FS welded specimen. So the more strength of the former specimen is reasonable. For FSW with vibration, the temperature is slightly higher than conventional FSW (Fig. 6) but the grain size due to effect of dynamic recovery and recrystallization is less than that (Table 2). According to Fig. 7, the strength of FS welded sample with vibration is higher than conventionally FS welded sample. During FSW with coolant and vibration, the decreasing effect of coolant on temperature is higher than increasing effect of vibration on temperature (Fig. 6). The decreasing effect of vibration on grain size is accompanied with decreasing effect of coolant on grain size. Based on the data in Table 2, grain size for FSW with coolant and vibration is at least among different welded specimens. Little precipitates dissolution due to presence of coolant as well as little grain size due to vibration make a desirable condition for strengthening. Based on the curves in Fig. 7, the strength of FS welded sample with coolant is higher than sample FS welded with vibration, although its ductility is lower.

One noticeable point in Fig. 7 is ductility increase as grain size decreases. It is believed that a high dislocation density allows a higher degree of plastic deformation and it provides a high ductility [31]. Schempp et al. [32] and Hansen [33] found via TEM that the grain boundaries increase the dislocation density through the generation of new dislocations called GNDs. They observed that ductility increased as grain size decreased. Spittle [34] noted that small grains have a higher resistance to crack propagation due to strain distribution between more grain boundaries. Estrin et al. [35] noted the possibility of ductility enhancement in AZ31 magnesium alloy due to the transition in the fracture mechanism from intergranular fracture to transgranular fracture as grain size decreases.

Formability index of studied specimens are presented in Fig. 9. Formability index which is a simple representative of toughness is determined by UTS × EL relation [36]. UTS and

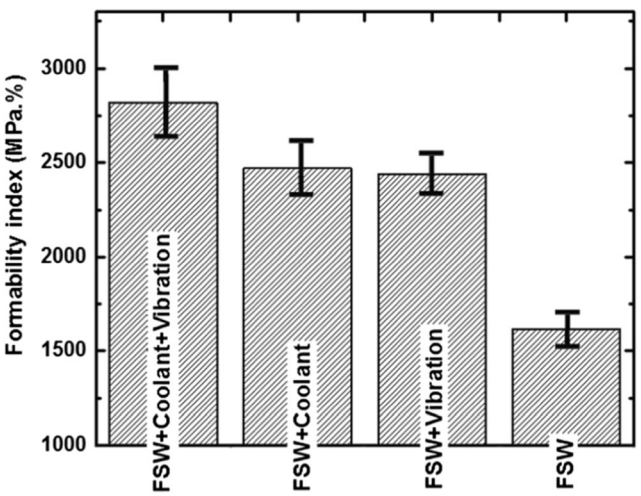

Fig. 9 Formability index of different specimens

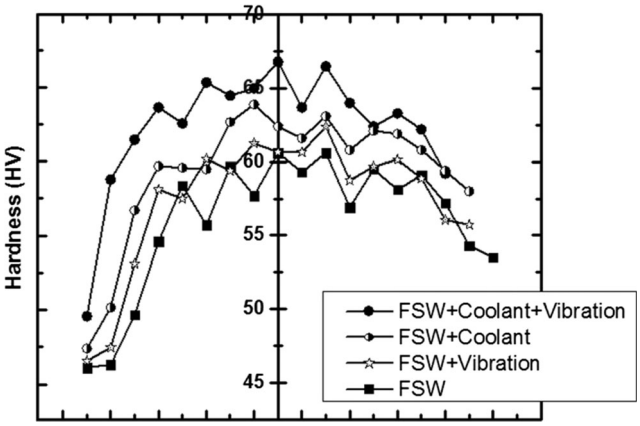

Fig. 10 Linear hardness profiles for different welding conditions

EL stand for ultimate tensile strength and elongation, respectively. It is observed that formability index of FS welded specimen with vibration and coolant is higher than those of other welded specimens. This can be related to higher strength and ductility of FS welded specimen with coolant and vibration with respect to other specimens.

Hardness measurement data for various zones of welded specimens are presented in Fig. 10. It is observed that hardness value of base material (100 HV) is higher than welded specimens. It is also observed that stir zone hardness of welded specimens is higher than that for HAZs. Cho et al. [9] noted that lower hardness of welded specimens of AA6061-T6 aluminum alloy with regard to base material is related to the decomposition of Mg_2Si precipitates during welding. Aluminum Al-Mg-Si systems are age-hardened alloys with {Mg, Si}-typed precipitates. Temperature during FSW is high enough to dissolve Mg_2Si precipitates and to decrease the hardness [9].

Higher hardness of stir zone with regard to HAZ can be related to grain size effect. It has been known that grain size for stir zone is normally lower than HAZ due to dynamic recovery and recrystallization which occur during FSW [14, 22]. As grain size decreases, due to increase in grain boundary volume fraction, the impediment to dislocation motion increases and correspondingly hardness increases [37]. Higher hardness of FS welded specimen using coolant and vibration with respect to other welded specimens may be related to presence of adequate volume fraction of Mg_2Si precipitations and low grain size. It was observed in Table 2 that presence of vibration and coolant during FSW led to significant decrease in grain size. Additionally, low dissolution of precipitates was characteristic of these specimens (Fig. 8). In this regard, more hardness for this specimen is inevitable.

4 Conclusions

AA6061-T6 aluminum alloy is a precipitation-hardened aluminum alloy, containing magnesium and silicon as its major alloying elements. It is one of the most common alloys of aluminum for general-purpose use. Different characteristics of AA6061 depend greatly on the heat treatment. Loss of strength after friction welding is a common problem for AA6061-T6 aluminum alloy. In the current research, a new method was presented to retrieve the strength loss during FSW. Joining workpieces were vibrated normal to weld line during FSW while a water circuited fixture was applied to fix the workpieces. The results showed that the stir zone grain size decreased as new method was applied. It was also concluded that the strength and hardness of FS welded specimen were improved as new method was applied. It was also observed that the ductility increased as FSW took place with application of vibration and coolant simultaneously. Application of this modified version of FSW is recommended for industries.

References

1. Abbasi M, Abdollahzadeh A, Bagheri B, Omidvar H (2015) The effect of SiC particle addition during FSW on microstructure and mechanical properties of AZ31 magnesium alloy. J Mater Eng Perform 24:5037–5045
2. Çam G, Mistikoglu S (2014) Recent development in friction stir welding of Al-alloys. J Mater Eng Perform 23:1936–1953
3. ASM Handbook vol. 2, "Properties and selection: nonferrous alloys and special-purpose materials", ASM International, USA, 1990
4. Sadeesh P et al (2014) Studies on friction stir welding of AA2024 and AA 6061 dissimilar metals. Procedia Engineering 75:145–149
5. Zhang Z, Zhang HW (2014) Solid mechanics-based Eulerian model of friction stir welding. International Journal of Advanced Manufacturing 72:1647–1653
6. Mofid MA, Abdollah-zadeh A, Ghaini FM (2012) The effect of water cooling during dissimilar friction stir welding of Al alloy to Mg alloy. Mater Des 36:161–167
7. Zhang HJ, Liu HJ, Yu L (2012) Effect of water cooling on the performances of friction stir welding heat-affected zone. J Mater Eng Perform 21:1182–1187
8. Sharma C, Dwivedi DK, Kumar P (2012) Influence of in-process cooling on tensile behavior of friction stir welded joints of AA7039. Mater Sci Eng A 556:479–487
9. Cho JH, Han SH, Lee CG (2016) Cooling effect on microstructure and mechanical properties during friction stir welding of Al-Mg-Si aluminum alloys. Mater Lett 180:157–161
10. Fratini L, Buffa G, Shivpuri R (2010) Mechanical and metallurgical effects of in process cooling during friction stir welding of AA7075-T6 butt joints. Acta Mater 58:2056–2067
11. M. Pitschman, J. W. Dolecki, G.W. Johns, J. Zhou, J.T. Roth, "Application of electric current in friction stir welding", Proceedings of the ASME 2010 International Manufactuing science and engineering conference MSEC2010, October 12–15, 2010, Pennsylvania, USA
12. Campanelli SL, Casalino G, Casavola C, Moramarco V (2013) Analysis and comparison of friction stir welding and laser assisted friction stir welding of aluminum alloy. Materials 6:5923–5941
13. Amini A, Amiri MR (2014) Study of ultrasonic vibrations' effect on friction stir welding. Int J Adv Manuf Technol 73:127–135

14. Rahmi M, Abbasi A (2017) Friction stir welding process: modified version of friction stir welding process. Int J Adv Manuf Technol 90:141–151
15. ASTM (2011) E3–11, "Standard guide for preparation of metallographic specimens". ASTM International, West Conshohocken, PA
16. ASTM-E8, "Standard test methods of tension testing of metallic materials", ASTM International, West Conshohocken, Pa, 2016
17. ASTM (2011) E384–11, "Standard test method for Knoop and Vickers hardness of materials". ASTM International, West Conshohocken, PA
18. ASTM-E112–13, "Standard test methods for determining average grain size", ASTM International, West Conshohocken, PA, 2013
19. Sarkari Khorrami M, Kazeminezhad M, Kokabi AH (2012) Mechanical properties of severely plastic deformation aluminum sheets joined by friction stir welding. Mater Sci Eng A 543:243–248
20. Jata KV, Semiatin SL (2010) Continuous dynamic recrystallization during friction stir welding of high strength aluminum alloys. Scr Mater 43:743–749
21. Kaibyshev R, Shipilova K, Musin F, Motohashi Y (2005) Continous dynamic recrystallization in an Al-Li-Mg-Sc alloy during equal-channel angular extrusion. Materials Science & Engineering A 396:341–351
22. Fouladi S, Abbasi M (2017) The effect of friction stir vibration welding process on characteristics of SiO2 incorporated joint. J Mater Process Technol 243:23–30
23. Li YS, Zhang Y, Tao NR, Lu K (2009) Effect of the Zener-Hollomon parameter on the microstructure and mechanical properties of Cu subjected to plastic deformation. Acta Mater 57:761–772
24. Chang CI, Lee CJ (2008) Relationship between grain size and Zener-Hollomon parameter during friction stir processing in AZ31 Mg alloys. Scr Mater 51:509–514
25. Liu G, Murr LE, Niou CS, McClure JC, Vega FR (1997) Microstructural aspects of the friction-stir welding of 6061-T6 aluminum. Scr Mater 37:355–361
26. Doos GM, Wahab BA (2012) Experimental study of friction stir welding of 6061-T6 aluminum pipe. International Journal of Mechanical Engineering and Robotics Research 1:143–156
27. Abdollahzadeh A et al (2017) "Structural evaluation and mechanical properties of AZ31/SiC nano-composite produced by friction stir welding process at various welding speeds", Proceedings of the institution of mechanical engineers, part L: Journal of Materials: Design and Application. doi:10.1177/1464420717708485
28. Dieter GE (1988) Mechanical metallurgy. McGraw-Hill Book Company, Singapore
29. Wu Q, Zhang Z (2017) Precipitation-induced grain growth simulation of friction-stir-welded AA6082-T6. Journal of Materials Engineering and Performance. doi:10.1007/s11665-017-2639-1
30. Jafari M, Abbasi M, Poursina D, Gheysarian A, Bagheri B (2017) Microstructures and mechanical properties of friction stir welded dissimilar steel-copper joints. J Mech Sci Technol 31:1135–1142
31. Callister WD (2007) Materials science and engineering: an introduction. Wiley, USA
32. Schempp P, Cross CE, Hacker R, Pittner A, Rethmeier M (2013) Influence of grain size on mechanical properties of aluminum GTA weld metal. Weld World 57:293–304
33. Hansen N (1977) The effect of grain size and strain on the tensile flow stress of aluminum at room temperature. Acta Metall 25:863–869
34. Spittle JA, Cushway AA (1983) Influence of superheat and grain structure on hot-tearing susceptibilities of Al-Cu alloy castings. Metals Technology 10:6–13
35. Estrin YZ et al (2010) Low temperature plastic deformation of AZ31 magnesium alloy with different microstructures. Low Temperature Physics 36:1100–1112
36. Gheysarian A, Abbasi M (2017) The effect of aging on microstructure, formability and springback of Ti-6Al-4V titanium alloy. J Mater Eng Perform 26:374–382
37. Naderi M, Abbasi M, Saeed-Akbari A (2013) Enhanced mechanical properties of a hot-stamped advanced high-strength steel via tempering treatment. Metallurgical and Materials Transactions 44A:1852–1861